Biobased chemicals from the catalytic depolymerization of Kraft lignin using supported noble metal-based catalysts

Hita, José Carlos; Deuss, P. J.; Bonura, G.; Frusteri, F.; Heeres, H. J.

Published in:
Fuel processing technology

DOI:
10.1016/j.fuproc.2018.06.018

Publication date:
2018

Fuel Processing Technology 179 (2018) 143–153

Contents lists available at ScienceDirect

Fuel Processing Technology

journal homepage: www.elsevier.com/locate/fuproc

Research article

Biobased chemicals from the catalytic depolymerization of Kraft lignin using supported noble metal-based catalysts

I. Hita[a,*], P.J. Deuss[a], G. Bonura[b], F. Frusteri[b], H.J. Heeres[a,**]

[a] Chemical Engineering Department (ENTEG), University of Groningen, Nijenborgh 4, 9747, AG, Groningen, the Netherlands
[b] CNR-ITAE, Istituto di Tecnologie Avanzate per l'Energia "Nicola Giordano", Via S. Lucia sopra Contesse, 5-98126 Messina, Italy

ARTICLE INFO

Keywords:
Hydrodeoxygenation
Depolymerization
Lignin
Noble metal
Alkylphenolics
Aromatics

ABSTRACT

Kraft lignin, a side-product of the paper industry, is considered an attractive feedstock for the production of biorenewable chemicals. However, its recalcitrant nature and sulfur content render catalytic conversions challenging. This study demonstrates the efficacy of noble metal-based catalysts for the production of a lignin oil enriched in alkylphenolic and aromatic compounds, by a catalytic hydrotreatment of Kraft lignin without the use of an external solvent. Eight commercially available catalysts were evaluated using four different metals (Ru, Pt, Pd, Rh) on two supports (activated carbon and Al_2O_3). The product oils were extensively analyzed by means of GPC, GCxGC-FID, GC–MS-FID, and elemental analysis. The catalysts were characterized by various techniques (N_2 physisorption, NH_3-TPD, XRD and TEM) before and after reaction, and their physico-chemical properties were correlated with catalytic performance. Al_2O_3 as support gave better results than carbon as support in terms of lignin oil yield and composition, due to a combination of higher total acidity, mildly acidic sites and a mesoporous structure. The metallic phase also significantly affected product distribution. The best results were obtained using a Rh/Al_2O_3 catalyst, resulting in a lignin oil yield of 36.3 wt% on a lignin intake and a total monomer yield of 30.0 wt% on lignin intake including 15.3 wt% of alkylphenolic and 7.9 wt% of aromatic compounds, and with a sulfur content < 0.01 wt%.

1. Introduction

The International Lignin Institute (ILI) recently reported that between 40 and 50 mT of lignin are produced annually, mainly from the pulp and paper industry [1–3]. Lignins are typically regarded as waste products and almost exclusively used in industry for onsite energy (steam) production. Lignin depolymerization processes have attracted increasing research interest, and are particularly aiming for the production of biofuels and value-added chemicals [4]. Several approaches have been reported for the valorization of lignin, examples are enzymatic processes [5, 6], thermal or catalytic pyrolysis [7, 8], depolymerization using basic catalysts [9], or oxidative processes [4, 10]. These studies so far have mainly focused towards the use of sulfur-free (organosolv) lignins as the lignin source. However, the most commercially employed pulping technique is the Kraft process, which leads to the formation of a lignin which contains significant amounts of sulfur [11].

Among the catalytic transformations studied so far, reductive processes like catalytic hydrotreatment have shown potential for lignin valorization [3]. Abundant research is available regarding the catalytic hydrotreatment of lignins in the presence of a solvent [12–14]. However, this approach has some major drawbacks such as partial incorporation of the solvent or solvent fragments into the products and, when considering industrial feasibility, the need for an efficient solvent recycling strategy. For this reason, a catalytic hydrotreatment without the use of an external solvent may have considerable advantages [15, 16].

Our group has reported on the catalytic hydrotreatment of Kraft lignin using sulfided NiMo and CoMo catalysts over basic and acidic supports at 350 °C and 100 bar of initial H_2 pressure, obtaining lignin oils in yields of up to 48 wt% with a high concentration of alkylphenolics (> 15 wt% on lignin intake) [14]. Recently Agarwal et al., showed that when using more severe conditions (450 °C), sulfided iron-based catalysts also proved suitable to obtain lignin oils (> 34 wt% on lignin intake) with even higher concentrations of alkylphenolics and aromatics (> 17 wt% and > 8 wt%, respectively) [17]. Up to now, only the use of sulfided catalysts has been reported to be effective, but their major disadvantage is the necessity to use an external sulfur source for in-situ activation of the catalysts and to maintain catalyst activity. This inevitably leads to products which contain significant amounts of

* Corresponding author at: Department of Chemical Engineering, University of the Basque Country (UPV/EHU), P.O. Box 644, 48080 Bilbao, Spain.
** Corresponding author.
E-mail addresses: idoia.hita@ehu.eus (I. Hita), h.j.heeres@rug.nl (H.J. Heeres).

https://doi.org/10.1016/j.fuproc.2018.06.018
Received 11 May 2018; Received in revised form 24 June 2018; Accepted 24 June 2018
Available online 04 July 2018

sulfur. In this context, noble-metal based catalysts could offer potential advantages, as a sulfur source is not required for catalytic activation [18]. Nevertheless, noble metal based catalysts have shown to be prone to deactivation due to catalyst poisoning in the presence of significant amounts of sulfur [19, 20].

So far, noble metals have been widely applied for the catalytic hydrotreatment of pyrolysis oils aiming for high-quality fuel production [21–25]. However, in comparison, limited research has been reported on the catalytic hydrotreatment of lignins using such catalysts. To date, the hydrotreatment of model compounds and particularly monomerics using noble metals has been reported extensively and shown the potential of these catalysts for lignin valorization [18, 26, 27], but exploratory studies on real lignin feedstock are limited.

Concerning the use of sulfur-free technical lignins, Bengoechea et al. recently explored the use of Rh, Ru and Pd catalysts supported on Al_2O_3 for the hydrotreatment of such lignins in water/formic acid, achieving oil yields of up to 91.2 wt% with a high concentration of hydrodeoxygenated compounds [28]. Kloekhorst et al. reported good performance of Ru and Pd supported catalysts for the hydrotreatment of a sulfur free organosolv Alcell lignin to obtain lignin oil yields up to 78 wt % and total monomer yields of 22 wt% (on lignin oil basis) [29]. Another example is the use of Ru/C for the hydrotreatment of pyrolytic lignins, the lignin (water insoluble) fraction from pyrolysis oil, which has reported to give lignin oils enriched in alkylphenolics and aromatics [30–32].

When considering sulfur-containing lignins, Yang et al. proposed a one-pot catalytic hydrocracking strategy for Kraft lignin over noble metal based catalysts (Ru, Pt, Pd, Rh) using isopropanol as a solvent. They found that temperature was the most important process variable considering lignin oil yields of up to 47 wt% could be obtained at 330 °C [33]. The product oil was rich in oxygen-containing cyclic and acyclic saturated compounds, indicating excessive hydrogenation of the lignin oil, which represents a drawback when the main goal is to obtain aromatic building blocks.

To the best of our knowledge, research on the valorization of Kraft lignin via hydrotreatment using noble metal based catalysts without the use of an external solvent has not been reported to date, evidencing the novelty of this work. As such, the molten lignin and the products (in a later stage of the batch reaction), are used to dissolve/disperse the lignin source.

In the research reported here, the use of eight noble metal based catalysts (5 wt% metal loading) for the catalytic hydrotreatment of Kraft lignin aiming for the production of valuable platform chemicals is discussed. The focus has been mainly on the optimization of the lignin oil yield and the content of alkylphenolics and aromatic compounds like substituted benzenes. Four different metallic phases were used (Ru, Pt, Pd, and Rh) over two commercially available and economically viable supports with different physico-chemical properties (activated carbon and Al_2O_3). Catalytic activity was evaluated in terms of lignin oil yield and composition. Extensive characterization and analysis of the lignin oils has been carried out by means of a wide variety of techniques (GCxGC-FID, GC–MS-FID, GPC, HSQC NMR, among others). The catalysts before and after reaction have been characterized in detail using a variety of techniques to correlate their physico-chemical properties with catalyst performance. In addition, the regenerability of the spent Rh/Al_2O_3 catalyst has been explored using an oxidation protocol.

2. Experimental

2.1. Chemicals and feed

All the chemicals used in this study were of analytical grade and used without further purification. Indulin-AT (Kraft lignin) was from Meadwestvaco Specialty Chemical, USA. Indulin-AT is a purified form of Kraft pine lignin and does not contain hemicellulose. All noble metal catalysts (Ru/C, Ru/Al_2O_3, Pt/C, Pt/Al_2O_3, Pd/C, Pd/Al_2O_3, Rh/C and Rh/Al_2O_3) were acquired from Sigma Aldrich with a 5 wt% metal loading. Dichloromethane (DCM) and acetone (both purchased from Boom B.V.) were used as solvents for recovering the different product fractions. Hydrogen (> 99.99%, purchased at Hoek Loos) was used as the reaction gas. The reference gas used for identification of the permanent gases in the gas product was supplied by Westfalen Gassen Nederland B.V.

2.2. Catalyst characterization

The surface area, pore volume and pore distribution of the fresh and regenerated catalyst samples were measured by means of N_2 physisorption at 77 K and using a Micromeritics 2020 apparatus. Prior to analysis, samples (~100 mg) were degassed for 4 h at 180 °C in vacuum conditions for desorbing impurities.

Surface concentration of acidic sites was determined by using a linear quartz micro-reactor (*l*, 200 mm; *i.d.*, 4 mm) in a conventional flow apparatus operating both in continuous and pulse mode. Before TPD experiments, the catalyst samples (~100 mg) were reduced under hydrogen atmosphere at 500 °C for 30 min and then saturated for 30 min at 150 °C in a gas mixture containing 5 vol% NH_3/He (flow rate of 25 mL min^{-1}). Then, the samples were purged in helium flow until a constant baseline level was attained. TPD measurements were performed in the temperature range of 150–600 °C at a rate of 10 °C min^{-1} using helium (25 STP mL min^{-1}) as carrier flow. The evolved ammonia was detected by an online thermal-conductivity detector, calibrated by the peak area of known pulses of NH_3.

Transmission Electron Microscopy (TEM) images were acquired using a Philips CM12 microscope operated at an acceleration voltage of 120 kV. Prior to analysis, the samples were ultrasonically dispersed in ethanol and subsequently placed on a carbon coated copper grid.

X-Ray diffraction (XRD) was used to gain information about the crystallinity of the samples, using a Bruker D8 Advance diffractometer, operating at 40 kV and 40 mA using CuKα radiation (λ = 1,5544 Å). Data were collected using a coupled Theta-2Theta configuration in the 2–80° 2θ range with a step size of 0.02 and a scan time of 1 s.

2.3. Catalytic hydrotreatment of Kraft lignin and product analysis

The catalytic hydrotreatment of Kraft lignin was carried out in a stainless steel batch reactor (100 mL, Parr Instruments Co.) equipped with a Rushton-type turbine and surrounded by a metal block containing an electrical resistance for heating purposes and channels allowing the flow of cooling water, as described in a previous publication from our group [15]. The unit is provided with both temperature and pressure sensors which, during the experiments, allow for these variables to be monitored online and logged on a PC. The temperature of the liquid in the reactor is measured by a thermocouple placed in the center of the reactor close to the mechanical stirrer. Lignins typically start to melt at approximately 200 °C which, together with the heavy stirring used in the process (1200 rpm), ensures that the temperature of the reactive liquid phase at reaction conditions is essentially uniform.

In all the experiments, the reactor was loaded with 15 g of Kraft lignin and 0.75 g of catalyst. After loading the reactor, it was flushed 3–4 times with H_2 to expel air, and then pressurized to 180 bar for a leak test at room temperature. Subsequently, the H_2 pressure was set at 100 bar and stirring was started at 1200 rpm. After that, the reactor was heated up to 450 °C (catalyst reduction occurs in-situ) at an approximate rate of 10 °C min^{-1}, and time zero was set once the desired reaction temperature was reached. After 4 h, the reactor was cooled to room temperature (setpoint 25 °C) and the pressure at room temperature was recorded allowing determination of the total amount of H_2 consumed during the reaction. Gas products were collected in a 3 L Tedlar gas bag to determine its composition. Fig. 1 depicts the lignin hydrotreatment workup procedure. After reaction, an aqueous phase and an organic phase (lignin oil) were obtained. The lignin oil and

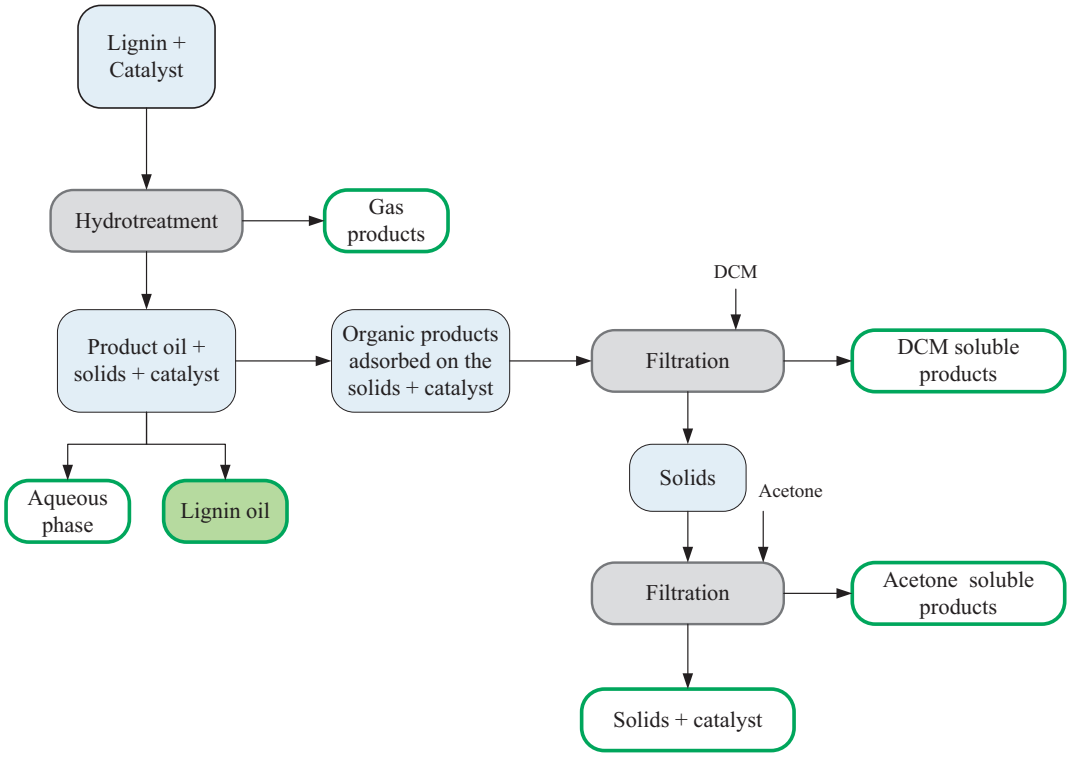

Fig. 1. Lignin hydrotreatment workup procedure.

water were easily separated from the rest of the products by decantation. After that, a solvent wash was used to recover the remaining organic products absorbed on the solid phase. It involves treatment of the solid phase with dichloromethane (DCM) and acetone, from where organic DCM and acetone soluble phases are respectively obtained. The remaining solid fraction, containing both the spent catalyst and the coke formed during reaction was dried and weighted for mass balance calculations.

Product yields and mass balance closures were calculated on a lignin intake basis, as specified in Eqs. (1) and (2), while carbon balances were calculated as shown in Eq. (3).

$$Product\ yield\ (wt\%) = \frac{Product\ weight\ (g)}{Lignin\ intake\ (g)} x\ 100 \quad (1)$$

$$Mass\ balance\ closure\ (wt\%) = \frac{\sum (Product\ weight\ (g))}{Lignin\ intake\ (g)} x\ 100 \quad (2)$$

$$Carbon\ balance\ closure\ (wt\%) = \frac{\sum C\ in\ products\ (g)}{C\ intake\ (g)} x\ 100 \quad (3)$$

The composition of the gas phase was analyzed by gas chromatography using a Hewlett Packard 5890 Series II GC apparatus equipped with a thermal conductivity detector (TCD), using a Porablot Q Al_2O_3/Na_2SO_4 column and a molecular sieve column (5 Å) connected in series. The reference gas had the following composition: 55.19% H_2, 19.70% CH_4, 3.00% CO, 18.10% CO_2, 0.51% ethylene, 1.49% ethane, 0.51% propylene and 1.50% propane.

Two-dimensional gas chromatography analyses were performed on the organic liquid product samples using a Trace GCxGC Interscience equipment provided with a flame ionization detector (GCxGC-FID), a cryogenic trap system, and two columns: a RTX-1701 capillary column (30 m × 0.25 mm i.d. and 0.25 μm film thickness) connected to a Rxi-5Sil MS column (120 cm × 0.15 mm i.d. and 0.15 μm film thickness). Helium was the carrier gas, and a dual jet modulator was used to trap the samples using CO_2 with a modulation time of 6 s. The injector temperature and FID temperature were set at 280 °C. The oven temperature was kept at 60 °C for 5 min and then heated to 250 °C with a rate of 3 °C min^{-1}. The pressure was set at 0.7 bar. Details on the calibration of the GCxGC-FID and relative response factors (RRFs) can be found in previous publications from our group [15, 29]. The percentage of GCxGC-detectables in the lignin oil was calculated using Eq. (4).

$$GC\ detectables\,(\%) = \frac{Total\ monomer\ yield\ (wt\%)}{Lignin\ oil\ yield\ (wt\%)} x\ 100 \quad (4)$$

For the identification of individual components in the lignin oil, gas chromatography analyses were performed using a Hewlett Packard 5890 GC provided with a FID detector, coupled with a Quadruple Hewlett Packard 6890 MSD (GC–MS-FID). The GC column was a RTX-1701 (60 m × 0.25 mm i.d. and 0.25 μm film thickness).

For both GCxGC-FID and GC–MS-FID analyses, the samples were diluted at a 1 : 30 ratio in tetrahydrofuran (THF, Boom B.V.) and then di-*n*-butylether (DBE, 99.3%, Sigma Aldrich) was added to serve as an internal standard. The identification of the main GCxGC components (aromatics, alkylphenolics, ketones, linear and cyclic alkanes, naphthenes, guaiacols and catecholics) was done by spiking with representative model compounds of the respective component groups and GC–MS-FID analysis.

The molecular weight distributions of the lignin oils, DCM and acetone soluble liquid fractions, were determined using gel permeation chromatography (GPC) analyses using a HP1100 unit equipped with three 300 × 7.5 mm PLgel 3 μm MIXED-E columns in series in combination with a GBC LC 1240 RI detector. THF was used as eluent (1 mL min^{-1}), toluene was added as a flow marker, and polystyrene standards with different molecular weight were used for calibration of the molecular weight.

The water content in the lignin oils has been determined by Karl-Fischer titration using a Metrohm Titrino 758 titration apparatus, and Hydranal® as solvent. Titrations were carried out using the Karl-Fischer titrant Composit 5 K (Riedel de Haen).

Total organic carbon (TOC) in the aqueous product was determined by means of a Shimadzu TOC-V_{CSH} TOC analyzer with an OCT-1

Table 1
Physico-chemical properties of the fresh noble metal based catalysts (as measured from N_2 adsorption-desorption isotherms at 77 K, NH_3 adsorption + TPD, and TEM).

	S_{BET} ($m^2\ g_{cat}^{-1}$)	V_{microp} ($cm^3\ g_{cat}^{-1}$)	Pore volume ($cm^3\ g_{cat}^{-1}$)	d_{pores} (Å)	NH_3 uptake (mmol g_{cat}^{-1})	Average metal particle size (nm)
Ru/C	674	0.155	0.685	84	0.102	2.2
Ru/Al_2O_3	84	0.002	0.210	98	0.134	14.2
Pt/C	1382	0.157	1.167	50	0.091	2.3
Pt/Al_2O_3	92	0.004	0.207	87	0.189	2.8
Pd/C	934	0.229	0.761	57	0.086	3.4
Pd/Al_2O_3	104	0.001	0.234	85	0.187	2.8
Rh/C	878	0.216	0.773	69	0.078	4.1
Rh/Al_2O_3	184	0.006	0.442	95	0.182	1.5

sampler port.

Elemental analyses (EA) were performed to determine the C, H, N, and S content in the lignin oils using an Euro Vector 3400 CHN-S analyzer. The amount of oxygen was calculated by the difference of CHNS. All analyses were carried out in duplicate and the average value was taken.

3. Results and discussion

3.1. Catalyst characterization

Eight noble metal catalysts were tested for the catalytic hydrotreatment of Kraft lignin in the absence of an external solvent, viz. Ru/C, Ru/Al_2O_3, Pt/C, Pt/Al_2O_3, Pd/C, Pd/Al_2O_3, Rh/C and Rh/Al_2O_3. The catalysts were characterized in detail by means of N_2 physisorption, isothermal NH_3-TPD, TEM and XRD analyses.

The main physico-chemical properties of the fresh catalysts are listed in Table 1. The N_2 physisorption analysis revealed clear differences regarding the textural properties of the catalyst (Fig. S1). All catalysts show type IV adsorption isotherms with a H1-type hysteresis loop, which is in agreement with literature data for similar carbon and alumina-based materials [34–36]. The observed H1-type hysteresis loop can be associated to a percolation effect caused by small metal oxide particles located inside the mesopores which might cause the formation of ink-bottle type pores [37]. As expected, much higher specific surface values were observed for the carbon-based catalysts (674–1382 $m^2\ g_{cat}^{-1}$) compared to the Al_2O_3 ones (84–184 $m^2\ g_{cat}^{-1}$). The carbon supports also proved to have a well-developed microporous structure with higher total pore (0.68–1.16 $cm^3\ g_{cat}^{-1}$) and micropore volumes (0.155–0.216 $cm^3\ g_{cat}^{-1}$) and, consequently, also narrower average pore diameters (50–84 Å). This microporosity is predominant in the case of the Pd/C and Rh/C catalysts, while Ru/C and Pt/C also present an important proportion of wider pores (see BJH pore volume distributions in Fig. S2). Interestingly, differences were observed between the Rh/Al_2O_3 catalyst and the other Al_2O_3-based catalysts, since the former had a specific surface and total pore volume which was double compared to the others.

The Al_2O_3 catalysts were by far more acidic (0.097–0.189 mmol g_{cat}^{-1}) than their carbon-based counterparts (0.078–0.102 mmol g_{cat}^{-1}). The acidity trends are Ru > Pt > Pd > Rh for the carbon-supported catalysts and Pt ≈ Pd ≈ Ru > Rh for the Al_2O_3-based catalysts. Two different types of acidic sites can be distinguished: (i) weak acidic sites (signal maxima at 297–367 °C) and (ii) strong acidic sites (signal maxima at 420–491 °C, Table S1, Fig. S3).

The relative amounts of the two types of acidic sites are very similar for the carbon-supported catalysts (56–68% weak vs. 44–32% strong acid sites), while significant variations are present for the Al_2O_3 catalysts. Here weaker sites are predominant in the Pt/Al_2O_3 and Rh/Al_2O_3 catalysts (61–64%) but stronger sites prevail in the Pd/Al_2O_3 catalyst (53%).

The XRD patterns of all the catalysts (Fig. S4) show very broad peaks, demonstrating the amorphous nature and low crystallinity of all the supports. In the case of the carbon supports, two prominent peaks are observed at around 26° and 43°, which are associated with the diffraction of the C(002) and C(100) planes of graphite, respectively [38]. Furthermore, characteristic peaks at 51° and 53° correspond to the C(102) and C(004) diffractions of graphite [39]. On the other hand, the alumina supported catalysts show characteristic peaks associated with the presence of both α-Al_2O_3 (peaks at 36°, 39° 57° and 66°) and γ-Al_2O_3 phases (peaks at 32° and 46°) [40].

TEM analyses were used to determine the morphology of the support and the metal particle size distribution (Table 1, Fig. S5). These images further confirm the amorphous nature of the supports as found by XRD. In all images, well-dispersed and homogeneously distributed metal nanoparticles can be distinguished. The average metal particle size is below 5 nm for all catalysts, except for the Ru/Al_2O_3 sample. Here, the average particle size is up to 14.2 nm and also a more heterogeneous particle distribution is observed. As a general trend, the metallic particles of the Al_2O_3 supported catalysts are slightly smaller compared to those deposited on the carbon support. The Rh/Al_2O_3 sample presents the smallest particles with an average size of 1.5 nm.

3.2. Catalytic hydrotreatment of Kraft lignin

Based on previous experience and aiming for full Kraft lignin conversion, the catalytic runs were carried out at 450 °C, 4 h of reaction time and 100 bar of initial H_2 pressure [17]. TGA analysis (Fig. S6) showed that Kraft lignin starts to decompose in the 200–420 °C range. Thus, reactions involving lignin are already expected to take place to a certain extent when heating up the reactor to the final temperature. Full conversion of the Kraft lignin was confirmed for all experiments by performing a dimethylsulfoxide (DMSO) extraction of the solid products after reaction. The initial amount of H_2 proved to be sufficient to ensure the availability of H_2 throughout the reaction. Each reaction was performed at least twice to determine reproducibility and the average values are provided.

Table 2 summarizes the obtained mass and carbon balances and product distributions together with the corresponding elemental compositions of the lignin oils. Satisfactory mass balance closures of > 90% were achieved in all cases. Carbon balances were also acceptable and > 86% in all cases.

After reaction, two liquid phases were obtained, an aqueous and an organic phase. During the work-up procedure, the organic phase was separated into three fractions, lignin oil and two fractions after washing the solids, viz., a DCM and acetone soluble liquid phase (Fig. 1). The lignin oil is the dominant fraction of the organic phase and accounts for at least 82% of the organic phase. When considering all products, the organic phase is the major product, with yields between 26.3 and 41.5 wt% on lignin intake, followed by the aqueous (20.1–22.0 wt%), solid (17.5–32.8 wt%) and gas products (9.5–15.2 wt%). Significant amounts of CH_4 (37.3–44.6 mol%), CO_2 (10.0–13.2 mol%) and ethane

Table 2
Product yields (wt% on lignin intake), mass and carbon balances, and elemental composition of the lignin oils obtained by the catalytic hydrotreatment of Kraft lignin using various noble metal catalysts.

	Ru/C	Ru/Al_2O_3	Pt/C	Pt/Al_2O_3	Pd/C	Pd/Al_2O_3	Rh/C	Rh/Al_2O_3
Organic phase (wt%)	36.2	30.4	26.3	40.3	29.7	37.5	39.2	41.5
Lignin oil (wt%)	31.7	26.5	21.5	35.2	25.1	33.3	33.8	36.3
DCM solubles (wt%)	4.2	3.6	4.6	4.6	4.3	3.8	4.8	5.0
Acet. Solubles (wt%)	0.3	0.3	0.2	0.5	0.3	0.4	0.6	0.2
Aqueous phase (wt%)	20.9	21.3	20.1	21.0	21.4	20.1	22.0	20.5
Gas (wt%)	15.0	13.5	12.3	14.4	13.3	15.2	14.6	14.5
Solid residue (wt%)	19.4	25.6	32.8	17.5	25.8	20.6	17.7	16.5
Mass balance (wt%)	91.6	90.7	91.5	93.5	90.3	93.4	93.5	92.9
C balance (wt%)	90.8	86.9	96.2	89.1	87.9	90.2	95.3	88.3
Elemental composition of the lignin oil (wt% on a dry basis)								
Carbon	81.8	82.0	80.2	81.7	79.4	79.8	81.7	81.3
Hydrogen	8.1	7.6	7.8	7.4	7.6	7.5	7.8	7.5
Oxygen	9.7	9.6	11.2	10.1	12.2	12.0	9.7	10.5
Nitrogen	0.3	0.6	0.7	0.7	0.7	0.6	0.7	0.7
Sulfur	0.01	0.1	0.15	0.05	0.01	0.06	0.07	< 0.01

(6.2–8.4 mol%) were formed during the reaction (Table S2). CH_4 is reported to be formed by the hydrogenolysis of O-Me groups, and also by gas phase reactions of CO and CO_2 with H_2 [29]. Clear enhancement in products yields are obtained through the catalytic approach in comparison with the thermal hydrotreatment (Table S3). Catalytic hydrotreatment using noble metal-based catalysts resulted in higher total organic phase yields (up to 30 wt%), with an enhanced selectivity towards lignin oil, and reduced gas and char yields. Furthermore, and in comparison with thermal Kraft lignin pyrolysis (500 °C), higher organic product yields were attained by the hydrotreatment approach, and also significantly lower char yields (18–33 wt% vs. 42–48 wt%) [41].

The product distribution (gas, liquids, solids) is affected by the nature of the catalyst. The highest lignin oil yield was achieved using Rh as the metallic phase for both alumina and carbon. As a general trend, the more acidic Al_2O_3-supported catalysts led to higher lignin oil yields and DCM and acetone soluble liquid fractions compared to the less acidic carbon supported counterparts.

When comparing the catalyst on the Al_2O_3 support series, the total organic yield is a function of the relative amount of weaker acidic sites in these catalysts (Fig. S7) for three of the catalysts (Pt/Al_2O_3, Pd/Al_2O_3 and Rh/Al_2O_3). This suggests that weak acidic sites play an important role in the chemistry and have a positive effect on the net rate of depolymerization reactions. Likely the acidity (in combination with the active metal) is sufficient to break relevant bonds in the lignin structure to lower molecular weight fragments but not too acidic to promote repolymerization reactions ultimately leading to char [42]. The worst performance considering the amounts of lignin oil was found for the Ru/Al_2O_3 catalyst and actually this catalyst does not fit in the trend that weak acid sites have a positive effect on lignin oil yields (Fig. S7). In this case, acidity is probably of less importance and catalyst activity is likely negatively affected by a poor metal nanoparticle dispersion (large average nanoparticle size of 14.2 nm, see Table 1 and Fig. S5).

The elemental composition of the lignin oils obtained for all catalysts are provided in Table 2. Compared to the Kraft lignin feed (62.2 wt % C, 29.8 wt% O, 6.0 wt% H, 1.2 wt% S, and 0.8 wt% N), a significant decrease in the amount of oxygen (9.7–12.2 wt%) and an increase in both carbon (79.4–82.0 wt%) and hydrogen (7.4–8.1 wt%) were observed, indicating that hydro(deoxy)genation reactions are occurring to a significant extent, as also proven by the Van Krevelen diagram in Fig. 2. The O/C ratio of the lignin oils (0.08–0.11) is considerably lower than for the Kraft lignin feed (0.36) and actually close to the typical O/C values for alkylphenolic compounds. When compared to (catalytic) pyrolytic strategies for industrial Kraft lignins, the catalytic hydrotreatment procedure leads to higher liquid product yields and lower gasification and water yields [41, 43], which is a clear advantage. The H/C ratio of the lignin oils (1.09–1.20) is about similar to that of Kraft

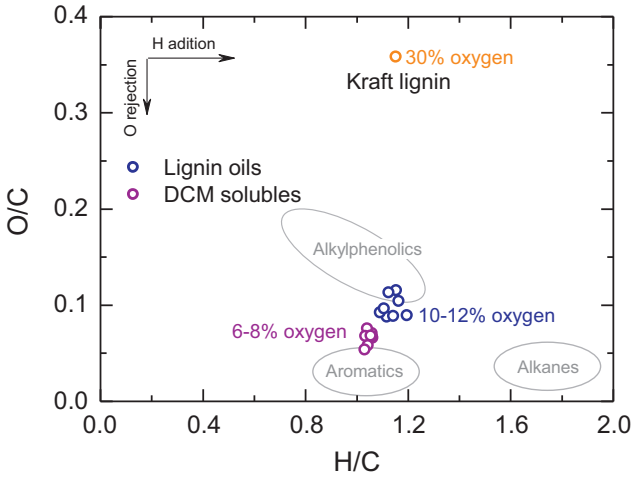

Fig. 2. Van Krevelen plot for Kraft lignin, lignin oils and DCM soluble fractions.

lignin (1.15). In all cases, but particularly for the Al_2O_3 supports, the lignin oils contain a very low sulfur content (even < 0.01 wt% using the Rh/Al_2O_3 catalyst).

The elemental composition of the DCM soluble fractions (Table S4) shows slightly higher amounts of carbon (83.3–84.2 wt%) and sulfur (0.1–0.3 wt%), while the amount of oxygen is lower (6.0–8.4 wt%) than that of the lignin oil. Fig. 2 also shows that the chemical compounds present in the DCM soluble fraction have a lower H/C ratio compared to the lignin oil, and present O/C ratios with values closer to the typical region for aromatic compounds (0.05–0.08). On the other hand, the solid products contain a much higher amount of oxygen (Table S5), and significantly higher amounts of sulfur. This implies that the sulfur-containing lignin fragments mainly end up in the solids fraction, presumably by condensation/repolymerization reactions. H_2S was also detected in the gas phase after reaction, though was not quantified.

The molecular weight distribution of Kraft lignin together with the lignin oil, DCM soluble and acetone soluble fractions obtained using the Rh/Al_2O_3 catalyst (the one that led to the highest lignin oil yield) are shown in Fig. 3. Compared with Kraft lignin, the product oils show a considerably narrowed molecular weight distribution, illustrating that depolymerization of lignin is occurring to a significant extent. Overall, very similar results were obtained for all the lignin oils and the DCM soluble fractions (Fig. S8), with average molecular weights in the ranges of 190–200 g mol^{-1} and 205–215 g mol^{-1}, respectively.

Furthermore, two-dimensional gas chromatography (GCxGC-FID) was used to determine the molecular composition of the lignin oil and

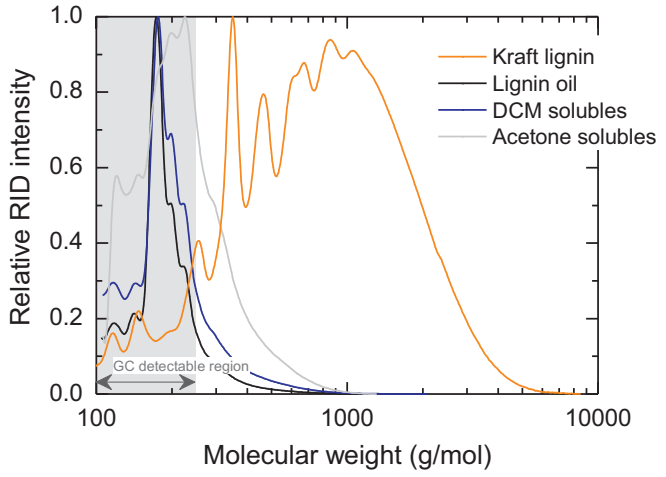

Fig. 3. Molecular weight distributions of the different liquid product fractions obtained using the Rh/Al_2O_3 catalyst.

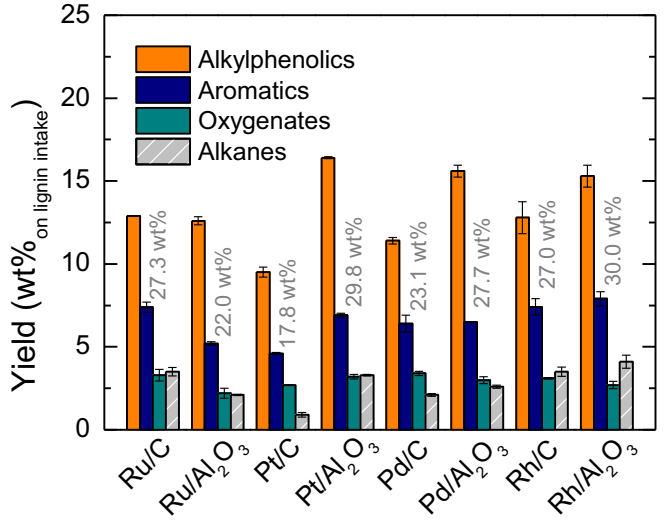

Fig. 4. Total monomer yields (% values) and composition of the lignin oils in terms of alkylphenolics, aromatics (monoaromatics and naphthalenes), oxygenates (guaiacols, catecholics and ketones) and alkanes (linear and cyclic) determined by 2D GCxGC (450 °C, 4 h, 100 bar H_2 initial pressure). The bars show the standard deviation obtained from 2 to 3 separate experiments.

DCM soluble fractions. GCxGC-FID has proven to be a suitable technique that allows quantification of component groups in complex organic mixtures [15, 34, 44]. The results for the lignin oil samples are summarized in Fig. 4 where the main chemical groups have been classified as: alkylphenolics, aromatics, oxygenated compounds and alkanes (see detailed composition in Table S6). Alkylphenolics are the dominant chemical group (11.4–16.4 wt%) in all the lignin oils together with aromatics (5.2–7.9 wt%), followed by oxygenates (2.2–3.4 wt%) and overall lower amounts of alkanes (0.9–4.1 wt%). The total monomer yields were between 22.0 and 30.0 wt% on a lignin basis. In combination with the lignin oil yields, this shows that 78–92% of the components in the lignin oil are of low molecular weight and detectable by GC (Table S7), in line with the GPC data. The relatively low presence of hydrogenated compounds (cyclohexanes, alkanes) should be highlighted, proving that noble metal-based catalysts are selective towards the formation of interesting phenolic and aromatic compounds.

Alkylphenolics were also the main chemical group in the DCM soluble product fraction (Table S8). These results are in agreement with the data shown in the van Krevelen plot in Fig. 2. The amount of detectable compounds in the DCM soluble fraction is between 67 and 78%

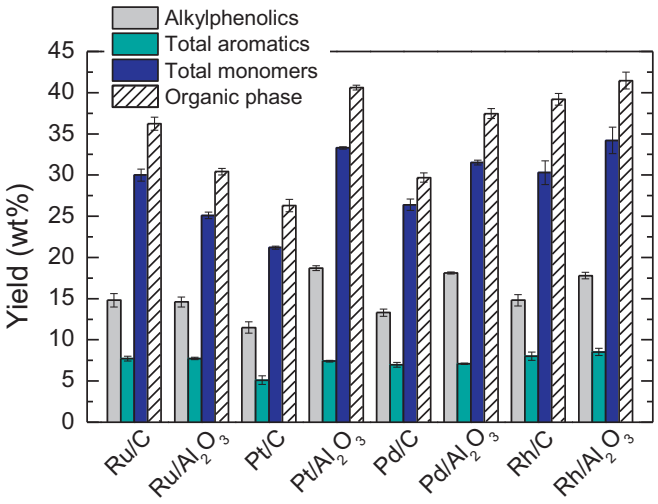

Fig. 5. Effect of the noble-metal based catalysts on the total yields (wt% on lignin intake) of organic phase, alkylphenolics, aromatics (including 1-ring structures and naphthalenes) and total monomers obtained in the organic products (lignin oil + DCM solubles). Error bars show the standard deviation obtained from 2 to 3 separate experiments.

(Table S6), which is lower in comparison with the lignin oils. This implies that the DCM soluble fraction contains a higher proportion of oligomeric compounds, which cannot be measured by GCxGC-FID techniques, in line with the GPC data (Fig. 3).

These results indicate that a greater depolymerization degree and a significantly higher amount of lighter chemical compounds (mainly alkylphenolics) in the lignin oil can be attained through a solvent-free depolymerization approach when compared to lignin pyrolysis [45, 46]. Recently, an efficient way of directing the pyrolysis product mixture towards lighter alkylphenolic compounds was reported by de Wild. et al. [47] using a 2-step pyrolysis + HDO strategy for different technical lignins using a NiMo catalyst for the second HDO step. However, the overall yield of alkylphenolics based on lignin intake for this two-step approach is half of that obtained with the catalytic hydrotreatment procedure reported here, showing the potential of the one-step hydrotreatment process.

For a proper comparison of the individual catalysts used in this study, the organic product yields, total monomers, and the amount of alkylphenolic and aromatic compounds in the whole organic product fraction (lignin oil and DCM soluble fractions assessed together) will be considered, and an overview of the data is given in Fig. 5. When comparing the supports, it appears that Al_2O_3 is preferred, as the total organic product yields (sum of the lignin oils, DCM and acetone solubles) are higher than those obtained for the carbon counterparts (30–42 wt% vs 26–39 wt% on lignin intake). Possible explanations are the presence of particularly weaker acidic sites on the alumina support that are known to favor the formation of low molecular weight compounds by enhancing chain scission and ring opening reactions [28]. The wider average pore diameter of Al_2O_3 (predominantly mesoporous) compared to carbon (mostly a microporous material) may also play a role as it is expected to favor diffusion of larger reactant molecules inside the pore structure. The relatively poor performance of the Ru/Al_2O_3 catalyst compared to the Ru/C catalyst can be attributed to the differences in the average metal particle size, which is significantly larger for the Ru/Al_2O_3 catalyst.

Among the carbon supported catalysts, only the results obtained with Rh/C are comparable with those for the Al_2O_3-based counterpart. The high specific surface of this catalyst, together with a much better nanoparticle dispersion (the smallest of all, see Fig. S4) may be the reasons for the relatively good performance of the Rh/C catalyst.

The results also indicate that the presence of bound sulfur in the

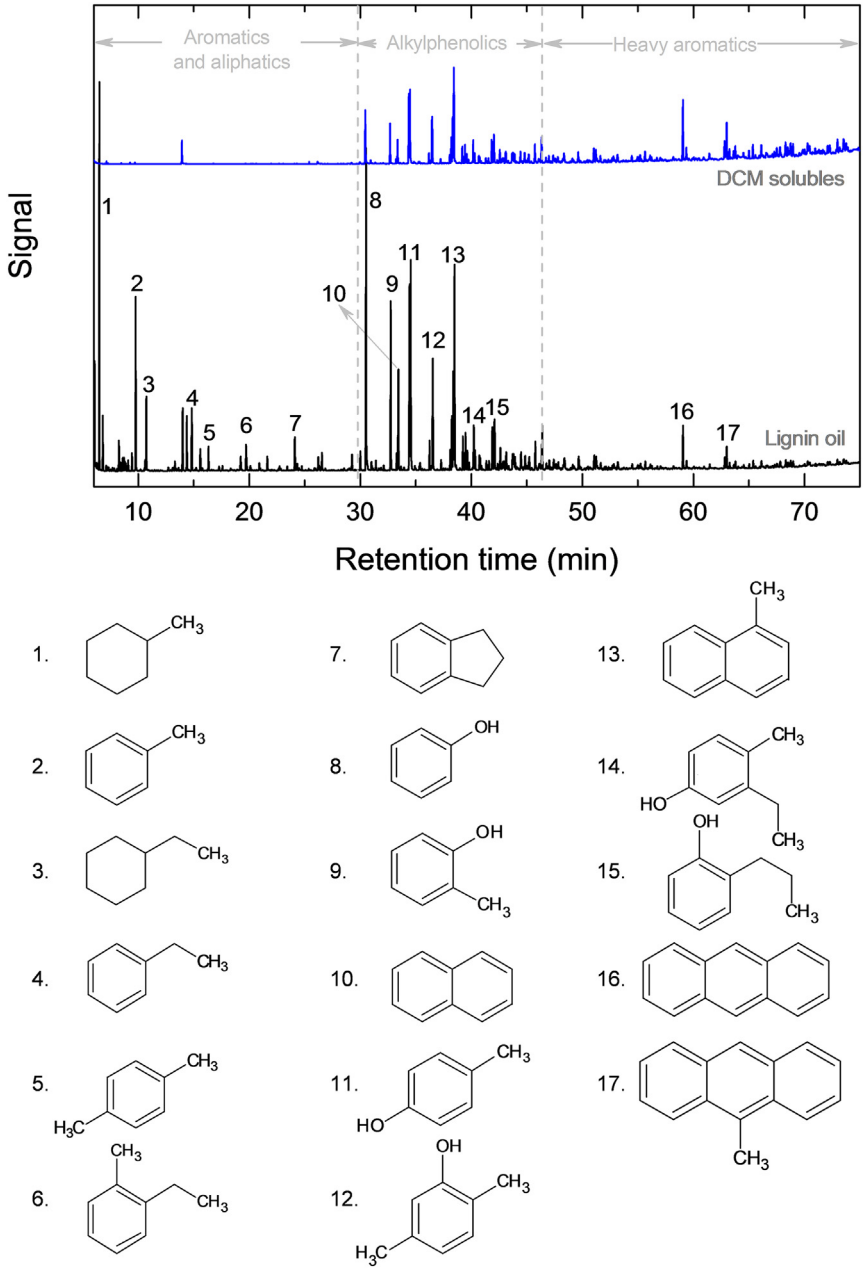

Fig. 6. GC–MS-FID chromatogram and main components of the lignin oils obtained using the Rh/Al_2O_3 catalyst.

Kraft lignin feed not necessarily results in inactive catalysts and, as with reactions in the absence of a catalyst, the formation of mainly solid products. However, it is difficult to quantitatively separate intrinsic activity of the individual catalysts and catalyst deactivation rates in the current experimental batch set-up. Some additional insights in catalyst stability have been obtained by performing catalyst recycle studies (vide infra).

In conclusion, the best catalyst performance regarding product distribution (organic yields and monomeric products) was achieved using the Rh/Al_2O_3 catalyst, likely due to favorable physico-chemical properties in terms of catalyst acidity (highest proportion of weaker acidic sites), surface area and metal particle size and dispersion. As such, in-depth characterization of the lignin oil obtained with this catalyst has been carried out and the results will be discussed in the upcoming section.

3.3. Detailed characterization of the lignin oil obtained with Rh/Al_2O_3

Representative GCxGC-FID chromatograms for the lignin oil and the DCM soluble fraction obtained using the Rh/Al_2O_3 catalyst are shown in Fig. S9. In both cases the higher intensity and abundance of the peak signals corresponding to alkylphenolic and aromatic compounds can be observed, evidencing the potential of both organic fractions as rich sources for biobased chemicals.

Identification of the main individual compounds in the product oil was performed using GC–MS-FID. Fig. 6 shows a representative chromatogram for the lignin oil and DCM solubles obtained with the Rh/Al_2O_3 catalyst. Data for the oils obtained with the other catalysts are given in Fig. S10. Three regions can be distinguished in the chromatogram based on the main components identified: (i) aromatics and aliphatics, (ii) alkylphenolics, and (iii) heavy aromatics. A detailed identification of individual components is given in Table S9. The lighter monomers in the lignin oil are mainly alkylated cyclic and aromatic

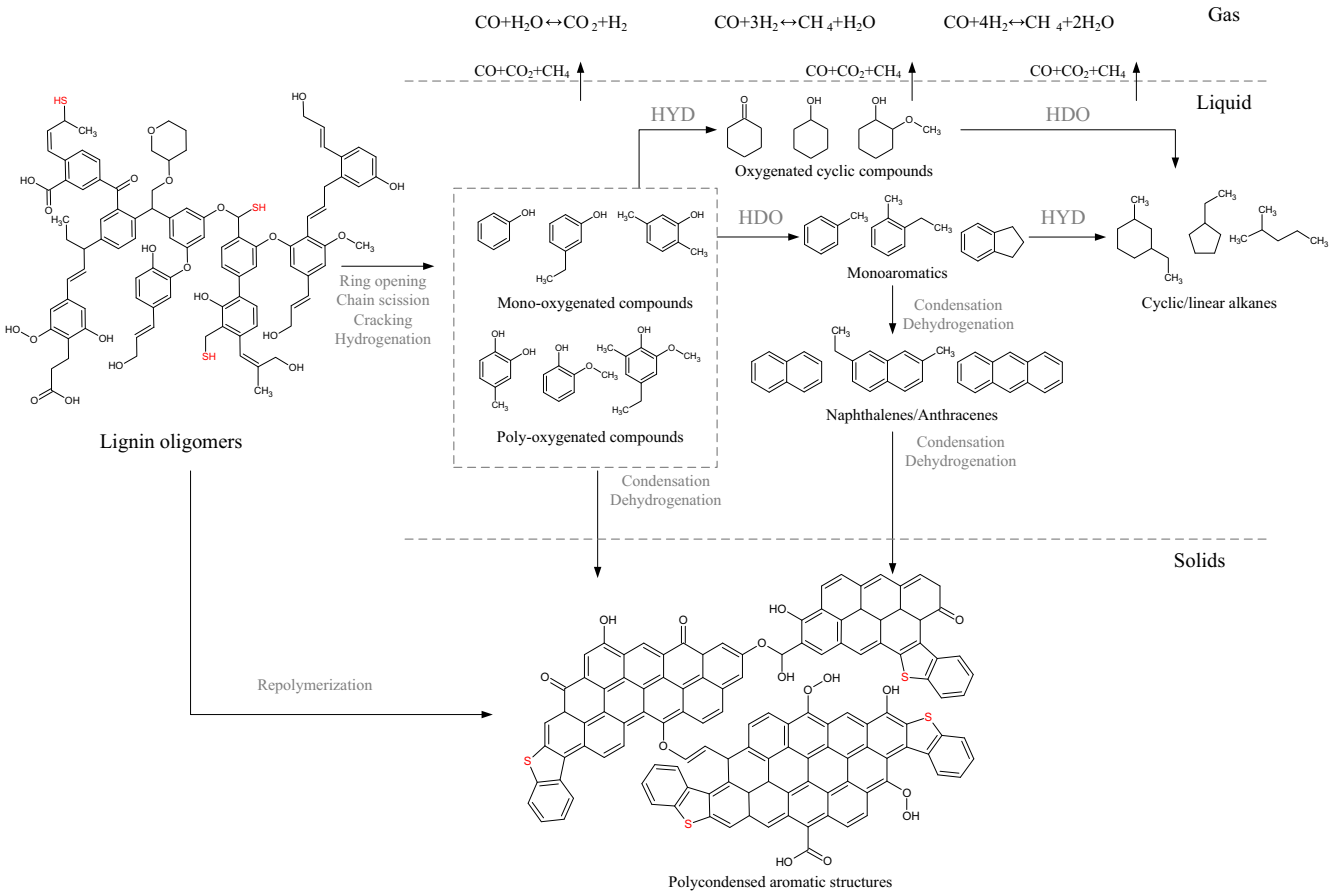

Scheme 1. Proposed reaction network for the hydrotreatment of Kraft lignin (adapted from Kloekhorst et al.) [29].

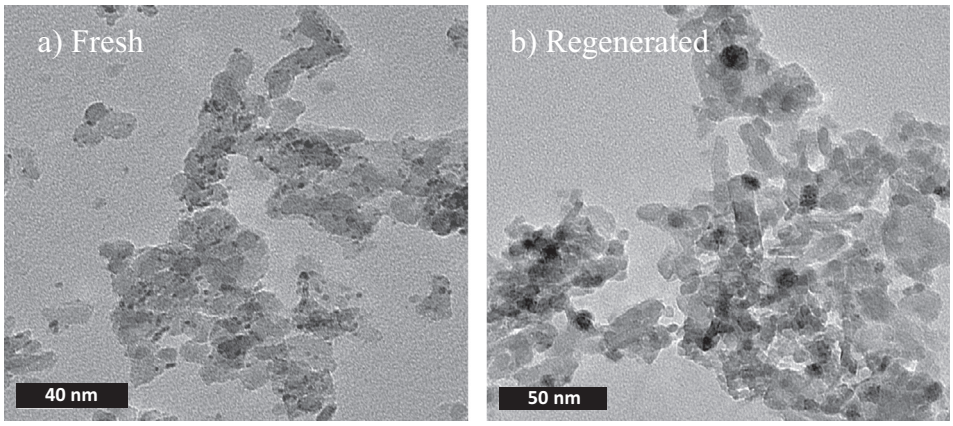

Fig. 7. TEM images of the a) fresh and b) regenerated Rh/Al_2O_3 catalysts.

compounds (mostly methylcyclohexane and toluene). Alkylphenolic compounds are the most abundant (phenol, 2-methylphenol, 4-methylphenol, 2,5-dimethylphenol). Smaller amounts of condensed bi- and tri-aromatics (alkylated naphthalenes and anthracenes) were detected, which potentially act as intermediates in the formation of solid products (heavily condensed and polymerized aromatic compounds) [48]. Concerning the DCM soluble product, lighter aromatics are about absent (in agreement with GCxGC-FID analysis) while the presence of heavier aromatics is prominent. Notably, alkylphenolics are again the main component class, in agreement with GCxGC-FID data.

3.4. Reaction network

A reaction network for the catalytic hydrotreatment of Kraft lignin is provided in Scheme 1. It is based on a previous proposal from our group for the hydrotreatment of Alcell lignin [29]. The alkylphenolics, guaiacols and catecholics likely originate from depolymerization of the lignin structure and successively formed lignin oligomers by either catalytic or thermal depolymerization processes involving cleavage of the various linkages. The presence of significant amounts of deoxygenated aromatic and naphthalenes in the organic products indicates that a fraction of the aforementioned oxygenated compounds react further. Two main routes are envisaged: (i) hydrogenation of unsaturated aromatics to form saturated oxygenated compounds like

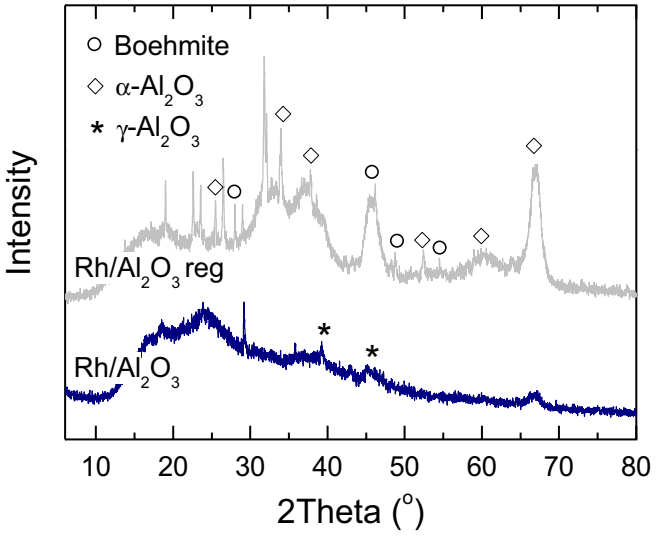

Fig. 8. XRD patterns of the fresh and regenerated Rh/Al_2O_3 catalyst.

alcohols or cyclic ketones and (ii) hydrodeoxygenation of oxygenated aromatics to produce aromatics, which can subsequently undergo further hydrogenation and ring opening reactions to form both cyclic and linear alkanes. The second route is predominant at our reaction conditions, as deduced from the concentrations reported in Fig. 4 and Table S8 (the amount of saturated oxygenated compounds was minor), and the elemental analysis of the lignin oils and DCM soluble fractions (Tables 2 and S4). Dehydrogenation and condensation reactions of monoaromatic compounds might also lead to the formation of higher aromatics like naphthalenes and anthracenes, which can also act as precursors in the formation of solids. The sulfur present in Kraft lignin, known to be mainly present as thiol groups [49], ends up mainly in the solids, which are likely heavy polyaromatic structures (as proven from the elemental analyses in Table S5).

3.5. Regenerability of the Rh/Al_2O_3 catalyst

The catalytic hydrotreatment of complex aromatic and oxygenated biofeeds is known to result in solids formation when operating at severe process conditions [24, 50]. Part of the solids are deposited on the catalytic surface and may result in catalyst deactivation. An oxidative treatment at elevated temperatures (500–600 °C) has been reported as an efficient strategy for the removal of the heavy carbonaceous species [42, 51]. The use of such an oxidative regeneration has been tested for the Rh/Al_2O_3 catalyst at a temperature of 550 °C (temperature ramp, 6 °C min^{-1} rate for 4 h). Afterwards, the catalyst was tested to evaluate its performance. The regenerated catalyst was also characterized by means of N_2 physisorption, NH_3-TPD and TEM. Characterization of the catalyst after a hydrotreatment reaction and before regeneration proved not possible because we were not able to separate the spent catalyst from the solid reaction products.

After regeneration of the catalyst, a significant decrease in the surface area (from 184 to 110 $m^2\ g_{cat}^{-1}$) and total volume (from 0.442 to 0.284 $cm^3\ g_{cat}^{-1}$) of catalyst was observed (see Fig. S11 for the isotherms), with barely no redistribution of the pore structure (Fig. S12). However, this did not lead to a significant increase of the average pore volume (95.2 to 94.1 Å). The decrease in surface area is likely related to pore occlusion during catalyst regeneration at high temperatures [52]. Total acidity dropped to half of the original value (from 0.182 to 0.097 mmol g_{cat}^{-1}) and a clear redistribution of acidic sites towards lower weaker acidity was observed (Fig. S13). The TEM images of the regenerated catalyst are given in Fig. 7. An increase in the average metal particle size from 1.5 nm for the fresh catalyst to 6.6 nm for the regenerated one was found, indicating the occurrence of active metal sintering. Interestingly, the regenerated catalyst still shows mainly well-dispersed smaller particles, together with some larger particles of around 20 nm.

The XRD analysis provided further information on the structural changes on the catalyst support (Fig. 8). While for the fresh catalyst pattern only small and broad peaks corresponding to the γ-Al_2O_3 and α-Al_2O_3 phases could be observed, much more sharp peaks appear in the pattern of the regenerated catalyst, also proving the formation of boehmite phase (AlOOH) as a consequence of the hydration of the

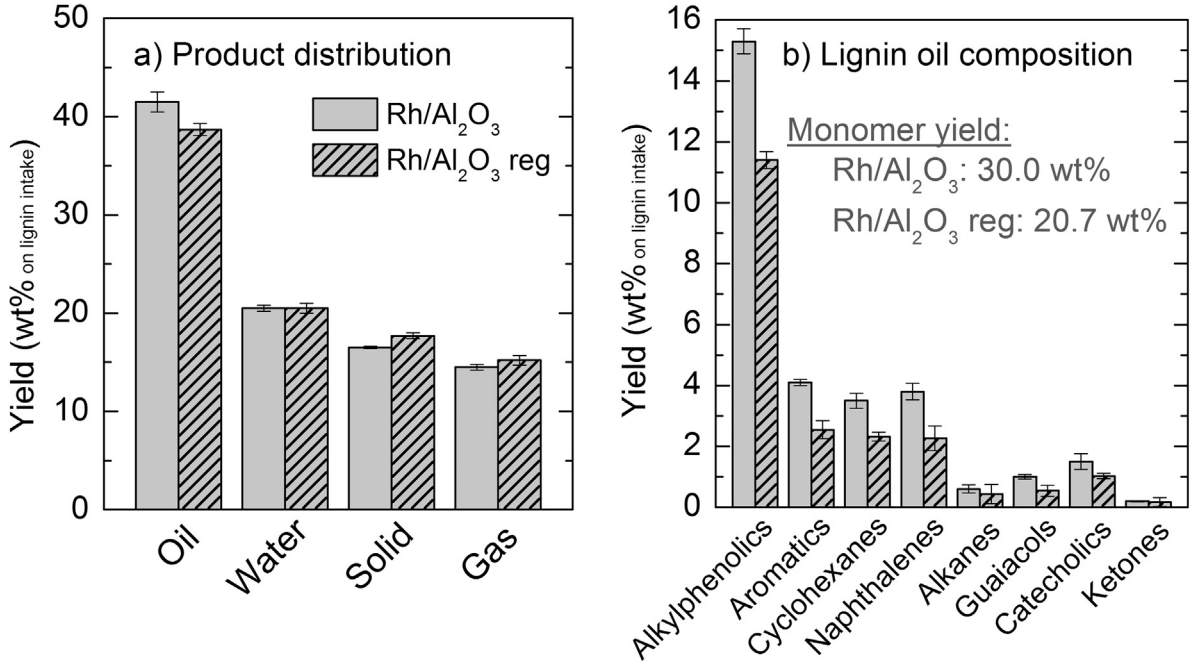

Fig. 9. Comparison between the performance of the fresh and regenerated Rh/Al_2O_3 catalyst in terms of a) product yield distribution and b) lignin oil composition. The bars show the standard deviation obtained from 2 experiments.

Al_2O_3 structure due to presence of water in the reaction media, formed in hydrodeoxygenation reactions.

The regenerated catalyst was tested for a standard catalytic hydrotreatment of Kraft lignin. Clear differences in performance of the fresh and regenerated catalyst were observed in terms of product yields and lignin oil composition (Fig. 9). Regarding product distribution (Fig. 9a), the regenerated catalyst shows a lower activity compared to the fresh catalyst (Tables 2), yielding 38.7 wt% of lignin oil, and slightly higher yields of solids (17.7 wt%) and gas (15.2 wt%), though the amounts of water formed (20.5 wt%) were similar to the fresh catalyst. As for product composition (Fig. 9b), a lower concentration of all the chemical groups was measured in the lignin oil, with 11.4 wt% of alkylphenolics, 5.3 wt% of total aromatics, 2.3 wt% of cyclohexanes, 1.0 wt% of catecholics and smaller amounts of alkanes, guaiacols and ketones (0.2–0.5 wt%). In this case, the total monomer yield dropped to 20.7 wt % compared with the 30.0 wt% obtained using the fresh catalyst. GPC analysis shows very little differences between the lignin oils obtained with the fresh and regenerated catalysts (Fig. S14), though some tailing of the curves point out a slightly higher proportion of heavier molecules in the product oils obtained with the regenerated catalyst.

This drop of activity is in agreement with the regenerated catalyst characterization results. The observed decrease of the surface area (attributed to pore occlusion) of the catalyst implies that a lower amount of both metallic and acidic sites (as evidenced from the loss of total acidity in the catalyst in Fig. S13) are accessible for the reactant molecules. Additionally, the formation of the AlOOH phase with an anticipated lower reactivity of the –OH groups on the catalytic surface is also expected to result in lower catalytic activity in contrast to the original γ-Al_2O_3 structure [53]. However, despite a certain activity loss, still a high lignin oil yield has been achieved with the regenerated catalyst. This can be explained by the presence of small and well-dispersed metal particles on the regenerated catalyst surface (metal particle agglomeration not taking place in such a high extent) and also the redistribution of acidic sites towards an overall much weaker acidity (Fig. S13), which, based on the observation that acid sites with a low acidity have a positive effect on catalyst performance (Fig. S7), is beneficial. The lignin oil obtained with the regenerated catalyst shows almost identical relative compositions of the different chemical groups in comparison with the oil produced with the fresh catalysts (Table S10), which implies that despite a slightly worse performance in terms of lignin oil production, high quality lignin oils can also be produced from the regenerated catalyst, with very high concentrations of alkylphenolic and aromatic compounds.

4. Conclusions

This study has demonstrated the potential of noble metal-based catalysts for the catalytic hydrotreatment of Kraft lignin to obtain lignin with a high proportion of alkylphenolic and aromatic compounds. A series of noble metal-based catalysts with different metallic phases (Rh, Pt, Pd, Rh) and supports (activated carbon, Al_2O_3) were evaluated in terms of product yields and composition, and the results were used to select the best active metal-support combination regarding organic product, aromatics and alkylphenolics yields.

The performance of the alumina-based noble metal catalysts were in general better than for the carbon supported ones. These findings were rationalized by considering that alumina has i) a higher total acidity and particularly a larger amount of relevant weaker acid sites compared to that of carbon and ii) a mesoporous structure which facilitates transfer of larger lignin derived molecules. Ru and Rh catalysts were shown to be more effective than Pd and Pt. The most promising results were obtained using the Rh/Al_2O_3 catalyst, giving a lignin oil yield of 36.3 wt% and 5.0 wt% of DCM soluble products (on a lignin intake basis) both being rich in alkylphenolics and aromatics. Remarkably the sulfur content of the lignin oils was very low (< 0.1 wt%.) and the highest proportion of sulfur was found in the solid fraction after reaction (1–2 wt%).

Regeneration of the spent Rh/Al_2O_3 catalyst by means of an oxidative treatment to remove coke resulted in structural (boehmite phase formation due to the presence of water in the reaction media) and physico-chemical changes (i.e. metal particle sintering, decrease in specific surface and redistribution of acidic sites), though catalytic activity was still considerable after a first regeneration cycle.

The results obtained in this study may be used to further improve the catalytic depolymerization of sulfur rich lignins in terms of catalyst design (i.e. tuning support properties, adding a second metal to the catalyst). Further studies in a continuous setup and preferably at milder reaction conditions for extended times on stream are required for an in-deep comprehension of the effect of sulfur poisoning on the stability of the catalyst.

Acknowledgements

Leon Rohrbach, Jan Henk Marsman, Erwin Wilbers, Marcel de Vries and Anne Appeldoorn are acknowledged for their technical and analytical support. We also thank Hans van der Velde for performing the elemental analysis and ICP measurements, Zhenchen Tang for help with the TEM analysis and Dr. Shilpa Agarwal for stimulating discussions.

Funding sources

This research has received funding from the Italian Ministry of Economic Development within the framework of the Agreement MiSE-CNR “Ricerca di Sistema Elettrico” [III ADP PAR 2013 – 2014 – BIOENERGIA L1-WP1.2]. Dr. Idoia Hita is grateful for her Basque Government postdoctoral grant [grant number POS_2015_1_0035].

Appendix A. Supplementary data

Supplementary data to this article can be found online at https://doi.org/10.1016/j.fuproc.2018.06.018.

References

[1] International Lignin Institute, www.Ili-Lignin.com , Accessed date: February 2018.
[2] S. Laurichesse, L. Avérous, Chemical modification of lignins: towards biobased polymers, Prog. Polym. Sci. 39 (2014) 1266–1290.
[3] J. Zakzeski, P.C.A. Bruijnincx, A.L. Jongerius, B.M. Weckhuysen, The catalytic valorization of lignin for the production of renewable chemicals, Chem. Rev. 110 (2010) 3552–3599.
[4] A. Rahimi, A. Ulbrich, J.J. Coon, S.S. Stahl, Formic-acid-induced depolymerization of oxidized lignin to aromatics, Nature 515 (2014) 249–252.
[5] G.T. Beckham, C.W. Johnson, E.M. Karp, D. Salvachúa, D.R. Vardon, Opportunities and challenges in biological lignin valorization, Curr. Opin. Biotechnol. 42 (2016) 40–53.
[6] O.Y. Abdelaziz, D.P. Brink, J. Prothmann, K. Ravi, M. Sun, J. García-Hidalgo, M. Sandahl, C.P. Hulteberg, C. Turner, G. Lidén, M.F. Gorwa-Grauslund, Biological valorization of low molecular weight lignin, Biotechnol. Adv. 34 (2016) 1318–1346.
[7] C. Liu, J. Hu, H. Zhang, R. Xiao, Thermal conversion of lignin to phenols: relevance between chemical structure and pyrolysis behaviors, Fuel 182 (2016) 864–870.
[8] H.W. Lee, Y.-M. Kim, J. Jae, B.H. Sung, S.-C. Jung, S.C. Kim, J.-K. Jeon, Y.-K. Park, Catalytic pyrolysis of lignin using a two-stage fixed bed reactor comprised of in-situ natural zeolite and ex-situ HZSM-5, J. Anal. Appl. Pyrolysis 122 (2016) 282–288.
[9] J. Long, R. Shu, Z. Yuan, T. Wang, Y. Xu, X. Zhang, Q. Zhang, L. Ma, Efficient valorization of lignin depolymerization products in the present of NixMg1 − xO, Appl. Energy 157 (2015) 540–545.
[10] J. Dai, A.F. Patti, K. Saito, Recent developments in chemical degradation of lignin: catalytic oxidation and ionic liquids, Tetrahedron Lett. 57 (2016) 4945–4951.
[11] J.C. Carvajal, Á. Gómez, C.A. Cardona, Comparison of lignin extraction processes: economic and environmental assessment, Bioresour. Technol. 214 (2016) 468–476.
[12] L. Liguori, T. Barth, Palladium-Nafion SAC-13 catalysed depolymerisation of lignin to phenols in formic acid and water, J. Anal. Appl. Pyrolysis 92 (2011) 477–484.
[13] A. Kloekhorst, Y. Shen, Y. Yie, M. Fang, H.J. Heeres, Catalytic hydrodeoxygenation and hydrocracking of Alcell® lignin in alcohol/formic acid mixtures using a Ru/C catalyst, Biomass Bioenergy 80 (2015) 147–161.
[14] A. Narani, R.K. Chowdari, C. Cannilla, G. Bonura, F. Frusteri, H.J. Heeres, K. Barta, Efficient catalytic hydrotreatment of Kraft lignin to alkylphenolics using supported NiW and NiMo catalysts in supercritical methanol, Green Chem. 17 (2015) 5046–5057.

[15] C.R. Kumar, N. Anand, A. Kloekhorst, C. Cannilla, G. Bonura, F. Frusteri, K. Barta, H.J. Heeres, Solvent free depolymerization of Kraft lignin to alkyl-phenolics using supported NiMo and CoMo catalysts, Green Chem. 17 (2015) 4921–4930.
[16] D. Meier, R. Ante, O. Faix, Catalytic hydropyrolysis of lignin: influence of reaction conditions on the formation and composition of liquid products, Bioresour. Technol. 40 (1992) 171–177.
[17] S. Agarwal, R.K. Chowdari, I. Hita, H.J. Heeres, Experimental studies on the hydrotreatment of kraft lignin to aromatics and alkylphenolics using economically viable Fe-based catalysts, ACS Sustain. Chem. Eng. 5 (2017) 2668–2678.
[18] B. Güvenatam, O. Kurşun, E.H.J. Heeres, E.A. Pidko, E.J.M. Hensen, Hydrodeoxygenation of mono- and dimeric lignin model compounds on noble metal catalysts, Catal. Today 233 (2014) 83–91.
[19] M. Fang, R.A. Sánchez-Delgado, Ruthenium nanoparticles supported on magnesium oxide: a versatile and recyclable dual-site catalyst for hydrogenation of mono- and poly-cyclic arenes, N-heteroaromatics, and S-heteroaromatics, J. Catal. 311 (2014) 357–368.
[20] C. Xie, Y. Chen, M.H. Engelhard, C. Song, Comparative study on the sulfur tolerance and carbon resistance of supported noble metal catalysts in steam reforming of liquid hydrocarbon fuel, ACS Catal. 2 (2012) 1127–1137.
[21] S. Kadarwati, S. Oudenhoven, M. Schagen, X. Hu, M. Garcia-Perez, S. Kersten, C.-Z. Li, R. Westerhof, Polymerization and cracking during the hydrotreatment of bio-oil and heavy fractions obtained by fractional condensation using Ru/C and NiMo/Al_2O_3 catalyst, J. Anal. Appl. Pyrolysis 118 (2016) 136–143.
[22] X. Li, R. Gunawan, Y. Wang, W. Chaiwat, X. Hu, M. Gholizadeh, D. Mourant, J. Bromly, C.-Z. Li, Upgrading of bio-oil into advanced biofuels and chemicals. Part III. Changes in aromatic structure and coke forming propensity during the catalytic hydrotreatment of a fast pyrolysis bio-oil with Pd/C catalyst, Fuel 116 (2014) 642–649.
[23] J.A. Capunitan, S.C. Capareda, Hydrotreatment of corn stover bio-oil using noble metal catalysts, Fuel Process. Technol. 125 (2014) 190–199.
[24] T. Cordero-Lanzac, R. Palos, J.M. Arandes, P. Castaño, J. Rodríguez-Mirasol, T. Cordero, J. Bilbao, Stability of an acid activated carbon based bifunctional catalyst for the raw bio-oil hydrodeoxygenation, Appl. Catal. B Environ. 203 (2017) 389–399.
[25] S. Oh, U.-J. Kim, I.-G. Choi, J.W. Choi, Solvent effects on improvement of fuel properties during hydrodeoxygenation process of bio-oil in the presence of Pt/C, Energy 113 (2016) 116–123.
[26] A.A. Dwiatmoko, L. Zhou, I. Kim, J.-W. Choi, D.J. Suh, J.-M. Ha, Hydrodeoxygenation of lignin-derived monomers and lignocellulose pyrolysis oil on the carbon-supported Ru catalysts, Catal. Today 265 (2016) 192–198.
[27] W. Mu, H. Ben, X. Du, X. Zhang, F. Hu, W. Liu, A.J. Ragauskas, Y. Deng, Noble metal catalyzed aqueous phase hydrogenation and hydrodeoxygenation of lignin-derived pyrolysis oil and related model compounds, Bioresour. Technol. 173 (2014) 6–10.
[28] M. Oregui Bengoechea, A. Hertzberg, N. Miletić, P.L. Arias, T. Barth, Simultaneous catalytic de-polymerization and hydrodeoxygenation of lignin in water/formic acid media with Rh/Al2O3, Ru/Al2O3 and Pd/Al2O3 as bifunctional catalysts, J. Anal. Appl. Pyrolysis 113 (2015) 713–722.
[29] A. Kloekhorst, H.J. Heeres, Catalytic hydrotreatment of Alcell lignin using supported Ru, Pd, and Cu catalysts, ACS Sustain. Chem. Eng. 3 (2015) 1905–1914.
[30] A. Kloekhorst, J. Wildschut, H.J. Heeres, Catalytic hydrotreatment of pyrolytic lignins to give alkylphenolics and aromatics using a supported Ru catalyst, Catal. Sci. Technol. 4 (2014) 2367–2377.
[31] P. de Wild, R. Van der Laan, A. Kloekhorst, E. Heeres, Lignin valorisation for chemicals and (transportation) fuels via (catalytic) pyrolysis and hydrodeoxygenation, Environ. Prog. Sustain. Energy 28 (2009) 461–469.
[32] H. Ben, W. Mu, Y. Deng, A.J. Ragauskas, Production of renewable gasoline from aqueous phase hydrogenation of lignin pyrolysis oil, Fuel 103 (2013) 1148–1153.
[33] J. Yang, L. Zhao, S. Liu, Y. Wang, L. Dai, High-quality bio-oil from one-pot catalytic hydrocracking of Kraft lignin over supported noble metal catalysts in isopropanol system, Bioresour. Technol. 212 (2016) 302–310.
[34] I. Hita, A. Gutiérrez, M. Olazar, J. Bilbao, J.M. Arandes, P. Castaño, Upgrading model compounds and Scrap Tires Pyrolysis Oil (STPO) on hydrotreating NiMo catalysts with tailored supports, Fuel 145 (2015) 158–169.
[35] I. Hita, T. Cordero-Lanzac, A. Gallardo, J.M. Arandes, J. Rodríguez-Mirasol, J. Bilbao, T. Cordero, P. Castaño, Phosphorus-containing activated carbon as acid support in a bifunctional Pt–Pd catalyst for tire oil hydrocracking, Catal. Commun. 78 (2016) 48–51.
[36] J.J. Ternero-Hidalgo, J.M. Rosas, J. Palomo, M.J. Valero-Romero, J. Rodríguez-Mirasol, T. Cordero, Functionalization of activated carbons by HNO3 treatment: influence of phosphorus surface groups, Carbon N. Y. 101 (2016) 409–419.
[37] A. Tuel, L.G. Hubert-Pfalzgraf, Nanometric monodispersed titanium oxide particles on mesoporous silica: synthesis, characterization, and catalytic activity in oxidation reactions in the liquid phase, J. Catal. 217 (2003) 343–353.
[38] J.C. Lasjaunias, M. Saint-Paul, A. Bilušić, A. Smontara, S. Gradečak, A.M. Tonejc, A. Tonejc, N. Kitamura, Acoustic and thermal transport properties of hard carbon formed from C60 fullerene, Phys. Rev. B: Condens. Matter Mater. Phys. 66 (2002) 143021–1430211.
[39] M. Dudek, P. Tomczyk, K.L. Juda, R. Tomov, B.A. Glowacki, S. Batty, P. Risby, R. Socha, Comparison of the performances of DCFC fuelled with the product of methane RF plasma reforming and carbon black, Int. J. Electrochem. Sci. 7 (2012) 6704–6721.
[40] M. Vahtrus, M. Umalas, B. Polyakov, L. Dorogin, R. Saar, M. Tamme, K. Saal, R. Lõhmus, S. Vlassov, Mechanical and structural characterizations of gamma- and alpha-alumina nanofibers, Mater. Charact. 107 (2015) 119–124.
[41] K.G. Kalogiannis, S.D. Stefanidis, C.M. Michailof, A.A. Lappas, E. Sjöholm, Pyrolysis of lignin with 2DGC quantification of lignin oil: effect of lignin type, process temperature and ZSM-5 in situ upgrading, J. Anal. Appl. Pyrolysis 115 (2015) 410–418.
[42] I. Hita, E. Rodríguez, M. Olazar, J. Bilbao, J.M. Arandes, P. Castaño, Prospects for obtaining high quality fuels from the hydrocracking of a hydrotreated scrap tires pyrolysis oil, Energy Fuels 29 (2015) 5458–5466.
[43] J.A. Santana, W.S. Carvalho, C.H. Ataíde, Catalytic effect of ZSM-5 zeolite and HY-340 niobic acid on the pyrolysis of industrial Kraft lignins, Ind. Crop. Prod. 111 (2018) 126–132.
[44] J.H. Marsman, J. Wildschut, P. Evers, S. de Koning, H.J. Heeres, Identification and classification of components in flash pyrolysis oil and hydrodeoxygenated oils by two-dimensional gas chromatography and time-of-flight mass spectrometry, J. Chromatogr. A 1188 (2008) 17–25.
[45] L. Fan, Y. Zhang, S. Liu, N. Zhou, P. Chen, Y. Cheng, M. Addy, Q. Lu, M.M. Omar, Y. Liu, Y. Wang, L. Dai, E. Anderson, P. Peng, H. Lei, R. Ruan, Bio-oil from fast pyrolysis of lignin: effects of process and upgrading parameters, Bioresour. Technol. 241 (2017) 1118–1126.
[46] V.F. Wendisch, Y. Kim, J.-H. Lee, Chemicals from lignin: recent depolymerization techniques and upgrading extended pathways, Curr. Opin. Green Sustain. Chem. 14 (2018) 33–39.
[47] P.J. de Wild, W.J.J. Huijgen, A. Kloekhorst, R.K. Chowdari, H.J. Heeres, Biobased alkylphenols from lignins via a two-step pyrolysis – hydrodeoxygenation approach, Bioresour. Technol. 229 (2017) 160–168.
[48] B. Valle, P. Castaño, M. Olazar, J. Bilbao, A.G. Gayubo, Deactivating species in the transformation of crude bio-oil with methanol into hydrocarbons on a HZSM-5 catalyst, J. Catal. 285 (2012) 304–314.
[49] P. Korntner, I. Sumerskii, M. Bacher, T. Rosenau, A. Potthast, Characterization of technical lignins by NMR spectroscopy: optimization of functional group analysis by 31P NMR spectroscopy, Holzforschung 69 (2015) 807–814.
[50] Y. Li, C. Zhang, Y. Liu, S. Tang, G. Chen, R. Zhang, X. Tang, Coke formation on the surface of Ni/HZSM-5 and Ni-Cu/HZSM-5 catalysts during bio-oil hydrodeoxygenation, Fuel 189 (2017) 23–31.
[51] Y. Yoshimura, E. Furimsky, Oxidative regeneration of hydrotreating catalysts, Appl. Catal. 23 (1986) 157–171.
[52] Y. Li, Z. Wu, Deactivation and burning regeneration of coked acid catalysts in catalytic cracking process of biomass tar, Zhongguo Dianji Gongcheng Xuebao/Proceedings Chinese Soc. Electr. Eng. 34 2014, pp. 1297–1303.
[53] G. Lefèvre, M. Duc, P. Lepeut, R. Caplain, M. Fédoroff, Hydration of γ-alumina in water and its effects on surface reactivity, Langmuir 18 (2002) 7530–7537.